EEE3037 Nanotechnology Coursework

6420013

Part I
Quantum Engineering Design

1   Structure Design

In order to design a quantum well which emits light of wavelength 1.55µm, a well material must be chosen such that an interband electron transition emits photons of this wavelength.

This band gap energy can be found from the equation

$$E = hf$$

When considering photons, f can be substituted with

$$f = \frac{c}{\lambda}$$

Therefore in order to find the E in terms of wavelength

$$E = \frac{hc}{\lambda}$$

Returning to the specifications, this allows 1.55µm to be expressed as 1.28x10⁻¹⁹ J or approximately 0.800 eV.

This energy value will be the same as the total interband transition for the well from the first confined hole energy level to the first confined electron enery level,

$$E_{g,transition} = E_{1h} + E_g + E_{1e} \approx 0.800 \text{eV} \tag{1}$$

see figure 1.

E_g should be the dominant term in this equation and as such when investigating suitable materials the bulk band gap should be close to but lower than 0.8eV.
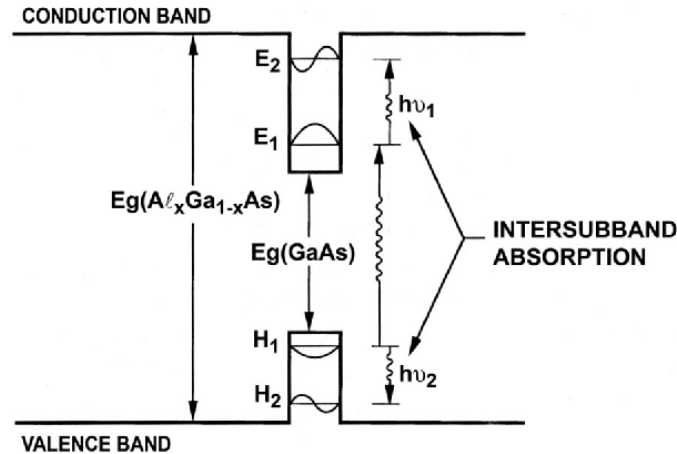

Figure 1: Band structure of an AlGaAs/GaAs/AlGaAs quantum well including discrete confined energy levels [1]

Material	Lattice Constant, α (Å)
InAs	6.0583
GaAs	5.6532
InP	5.8687

Table 1: Lattice constants for prospective well and barrier materials [2]

Material	Band Gap at 300K, E_g (eV)
InAs	0.35
GaAs	1.42
InP	1.34

Table 2: Band gaps for prospective well and barrier materials [2]

Ternary alloys were investigated in order to allow precise control over the lattice constants and band gap by varying the composition ratio.

Indium gallium arsenide ($In_xGa_{(1-x)}As$) as a well material with indium phosphide (InP) as a barrier material would provide a suitable combination assuming that a composition ratio x could be found that satisfied the two conditions of having the required bulk band gap and being lattice matched. A common ratio in industry is $In_{0.53}Ga_{0.47}As$ and as such this was tested first.

1.1 Lattice Match

Lattice matching is the process of ensuring that two crystalline structures are of similar dimensions in order to decrease strain at the interface between the two materials. This is particularly important for quantum wells formed through epitaxial growth as strain introduced between such thin layers can cause defects which ultimately negatively affect it's electronic properties.

The lattice constants between the barrier and well materials should be as close as is deemed acceptable for the application. The lattice constants for the prospective materials are shown in table 1.

In order to compute a compound lattice constant for InGaAs, Vegard's law can be applied. Vegard's law provides an approximation for the lattice constant of a solid solution by finding the weighted average of the individual lattice constants by composition ratio and is given by:

$$\alpha_{A_{(1-x)}B_x} = (1-x)\,\alpha_A + x\alpha_B$$

Applying this to the prospective well material gives the following,

$$\alpha_{In_{0.53}Ga_{0.47}As} = 0.53 \cdot 6.0583 + 0.47 \cdot 5.6532 = 5.8679$$

This shows that to 4 significant figures the composition of InGaAs is lattice matched to InP to within 0.001Å which is sufficient for this application.

1.2 Band Gap

Vegard's law can also be used to approximate the band gap of a ternary alloy, such as InGaAs. The band gaps at 300K for each alloy can be seen in table 2.

In this case the band gap approximates to,

$$E_{g,In_{0.53}Ga_{0.47}As} \approx 0.53 \cdot 0.35 + 0.47 \cdot 1.42 \approx 0.85\text{eV}$$

However the band gap has been experimentally found to be 0.75eV [3]. This implies that the linear relationship provided by Vegard's law is not accurate enough and in this case a modified version including a bowing parameter b should be used,

$$E_{g,total} = xE_{g,a} + (1-x)\,E_{g,b} - bx\,(1-x)$$

For this application, however, the experimentally determined value will be used. This value is ideal for this application as it is comparable to and slightly lower than the required 0.8eV energy value.

Charge Carrier	Effective mass ratio in $In_{0.53}Ga_{0.47}As$ ($\frac{m^*}{m^0}$)
Electron	0.041 [4]
Light Hole	0.051 [5]
Heavy Hole	0.2 [6]

Table 3: Effective masses of charge carriers in

1.3 Width Calculation

Having found two materials that are lattice matched with a suitable band gap value, the final calculation is that of the quantum well width. In order to calculate this value, the equation for confined energy levels within an infinite quantum well will be used,

$$E_n = \frac{n^2\pi^2\hbar^2}{2mL^2} \tag{2}$$

Referring back to equation 1, the terms for the first electron and hole energy levels can each be replaced with equation 2 as seen below,

$$E_{g,transition} = 0.8\text{eV} = E_{1h} + E_{g,InGaAs} + E_{1e} = \frac{1^2\pi^2\hbar^2}{2m_h^*L^2} + E_{g,InGaAs} + \frac{1^2\pi^2\hbar^2}{2m_e^*L^2}$$

With the experimentally determined value for $E_{g,,InGaAs}$ this equation becomes

$$0.8\text{eV} = \frac{\pi^2\hbar^2}{2m_h^*L^2} + 0.75\text{eV} + \frac{\pi^2\hbar^2}{2m_e^*L^2}$$

$$0.05\text{eV} = \frac{\pi^2\hbar^2}{2L^2}\left(\frac{1}{m_h^*} + \frac{1}{m_e^*}\right)$$

$$L = \sqrt{\frac{\pi^2\hbar^2}{2\cdot(0.05\text{eV})}\cdot\left(\frac{1}{m_h^*} + \frac{1}{m_e^*}\right)}$$

As a frequently studied composition due to it's favourable structural parameters with InP, The charge carrier effective masses of $In_{0.53}Ga_{0.47}As$ have been found experimentally to be as shown in table 3.

As the electrical and optical properties of the valence band are governed by the heavy hole interactions, this effective mass ratio will be used.

Substituting these ratios into the above provides,

$$L = \sqrt{\frac{\pi^2\hbar^2}{2\cdot(0.05\text{eV})\cdot m_e}\cdot\left(\frac{1}{0.2} + \frac{1}{0.041}\right)}$$

which reduces to a well length of 14.87nm.

1.4 Confined Energy Level Calculations

With all the parameters of the well ascertained the first and second confined electron and hole energy levels can be found by utilising equation 2.

For confined electron states:

$$E_{1e} = \frac{1^2\pi^2\hbar^2}{2\cdot m_e^*\cdot(14.87\text{nm})^2}$$

$$E_{1e} = 6.65 \times 10^{-21}\text{J} = 0.041\text{eV}$$

This equation shows that confiend energy level values are proportional to the square of n, the principal quantum number or energy level. As such:

$$E_{2e} = 2^2 \cdot E_{1e}$$

$$E_{2e} = 2.66 \times 10^{-20} \text{J} = 0.17 \text{eV}$$

For confined hole states:

$$E_{1h} = \frac{1^2 \pi^2 \hbar^2}{2 \cdot m_h^* \cdot (14.87 \text{nm})^2}$$

$$E_{1h} = 1.36 \times 10^{-21} \text{J} = 0.0085 \text{eV}$$

$$E_{2h} = 2^2 \cdot E_{1h}$$

$$E_{2h} = 5.45 \times 10^{-21} \text{J} = 0.034 \text{eV}$$

With the dimensions and first confined energy levels calculated, the final design for the quantum well can be seen in figure 2.

2   Probability Plot

The probability of finding an electron in a quantum well is given by

$$P = \int_0^L \psi^* \psi dx \tag{3}$$

with ψ in the case of an infinite quantum well being given by,

$$\psi(x) = A \sin(kx) = A \sin\left(\frac{n\pi}{L}x\right)$$

Here A acts as a normalisation constant to satisfy the conditions

$$\int_{allspace} \psi^* \psi dV = 1$$

in this case providing the wave function ψ as

$$\psi(x) = \sqrt{\frac{2}{L}} \sin\left(\frac{n\pi}{L}x\right) \tag{4}$$

Importantly, the above conditions are for an infinite quantum well where an assumption is made that the well has a barrier region of infinite potential such that the wavefunction is confined to the well. A real quantum well is unable to satisfy this leading to the wavefunction "spilling" into the barrier region. For the purposes of plotting the probability density, however, it is a reasonable assumption to make.

Considering equation 3, if the probability can be found by integrating $\psi^* \psi$, or in this situation ψ^2 then the probability can be shown by plotting ψ^2, see figure 3. Here the well stretches from 0 to the blue line along the x axis and n has been set to 1 for the ground state. This function for the first excited state can be seen in figure 4.
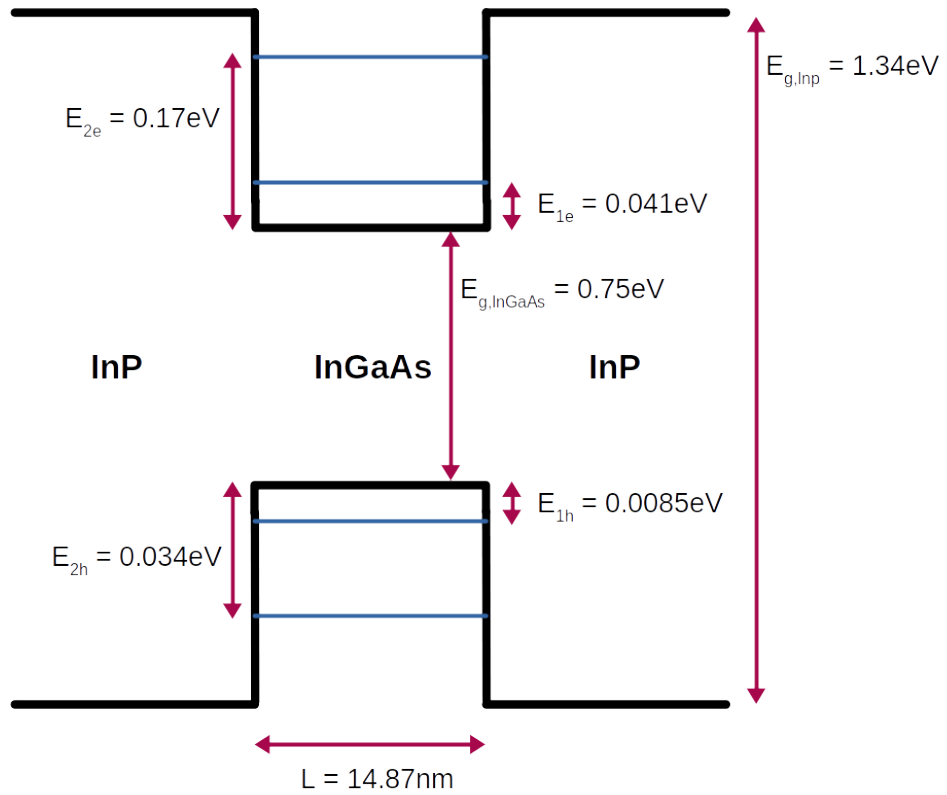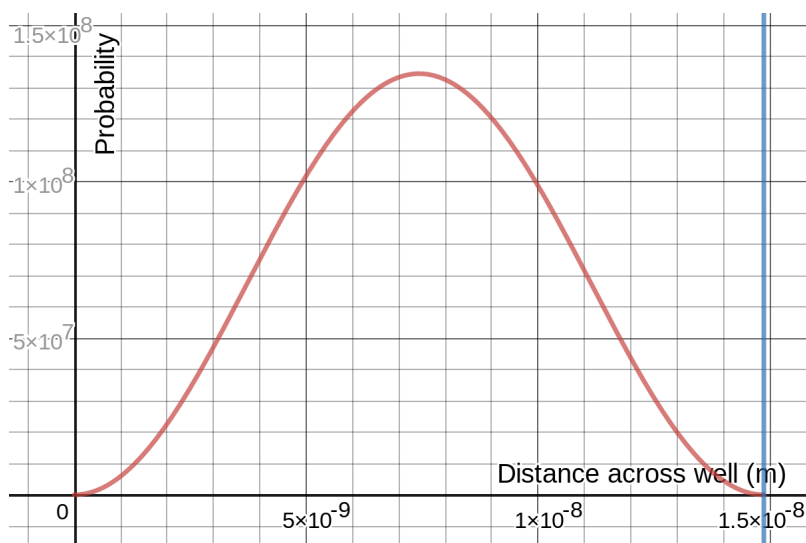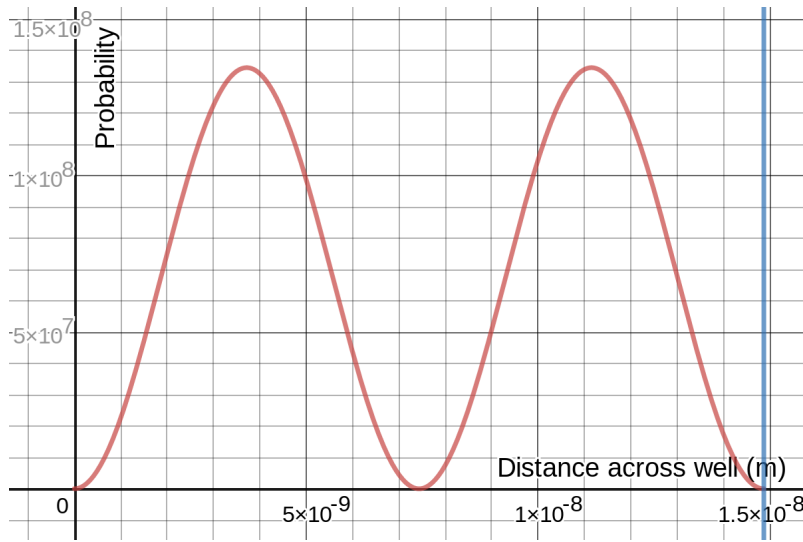
Figure 2: InP/InGaAs/InP quantum well design

Figure 3: Probability plot for electron in ground state

Figure 4: Probability plot for electron in 1$^{\text{st}}$ excited state

3   Probability Intervals

Combining equations 3 and 4 gives the final probability function for a distance across the well from $x = 0$ to $x = x_0$:

$$P\left(0 \leq x \leq x_0\right) = \frac{1}{L}\left(x_0 - \frac{L}{2n\pi}\sin\left(\frac{2n\pi x_0}{L}\right)\right)$$

For an arbitrary interval across the well, this becomes:

$$P\left(a \leq x \leq b\right) = \frac{1}{L}\left((b - a) - \frac{L}{2n\pi}\left(\sin\left(\frac{2n\pi b}{L}\right) - \sin\left(\frac{2n\pi a}{L}\right)\right)\right)$$

This equation can be utilised in order to find the probability of finding the electron between 2nm and 4nm and between 6nm and 8nm, the intervals for which can be seen plotted in figure 5.

3.1   2nm to 4nm

$$P\left(2\text{nm} \leq x \leq 4\text{nm}\right) = \frac{1}{L}\left(2\text{nm} - \frac{L}{2n\pi}\left(\sin\left(\frac{2n\pi\cdot(4\text{nm})}{L}\right) - \sin\left(\frac{2n\pi\cdot(2\text{nm})}{L}\right)\right)\right)$$

$$P\left(2\text{nm} \leq x \leq 4\text{nm}\right) = \frac{1}{14.87\text{nm}}\left(2\text{nm} - \frac{14.87\text{nm}}{2\pi}\left(\sin\left(\frac{2\pi\cdot(4\text{nm})}{14.87\text{nm}}\right) - \sin\left(\frac{2\pi\cdot(2\text{nm})}{14.87\text{nm}}\right)\right)\right)$$

$$P\left(2\text{nm} \leq x \leq 4\text{nm}\right) \approx 0.0955$$

3.2   6nm to 8nm

$$P\left(6\text{nm} \leq x \leq 8\text{nm}\right) = \frac{1}{L}\left(2\text{nm} - \frac{L}{2n\pi}\left(\sin\left(\frac{2n\pi\cdot(8\text{nm})}{L}\right) - \sin\left(\frac{2n\pi\cdot(6\text{nm})}{L}\right)\right)\right)$$

$$P\left(6\text{nm} \leq x \leq 8\text{nm}\right) = \frac{1}{14.87\text{nm}}\left(2\text{nm} - \frac{14.87\text{nm}}{2\pi}\left(\sin\left(\frac{2\pi\cdot(8\text{nm})}{14.87\text{nm}}\right) - \sin\left(\frac{2\pi\cdot(6\text{nm})}{14.87\text{nm}}\right)\right)\right)$$

$$P\left(6\text{nm} \leq x \leq 8\text{nm}\right) \approx 0.263$$

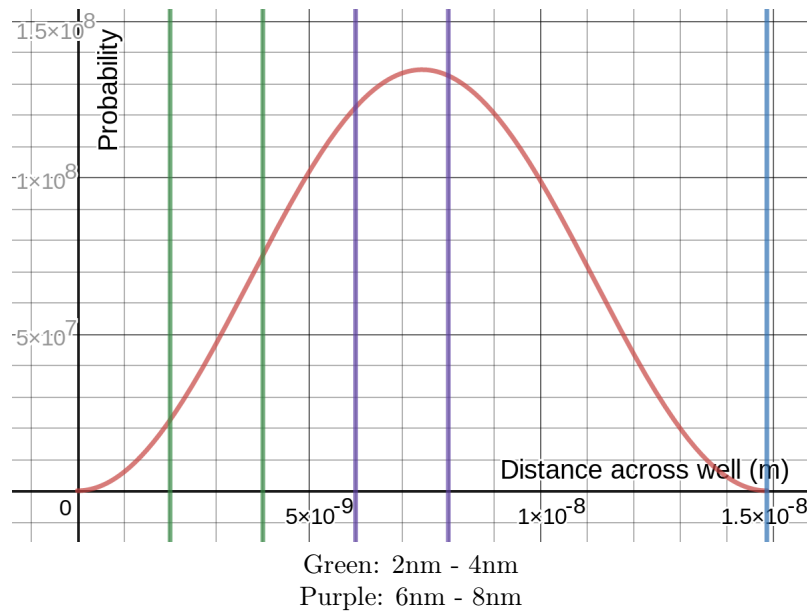Green: 2nm - 4nm
Purple: 6nm - 8nm

Figure 5: Probability plot for electron in ground state with distance intervals

3.3   Conclusions

Considering these two probabilities it is clear that it is more likely for the electron to be found between 6nm and 8nm than between 2nm and 4nm across the well. This is as expected considering 6nm to 8nm places the interval towards the center of the 14.87nm well. As the probability density function is a $\sin^2$ function, the maxium area will be towards the center. Referring to figure 5 this can be seen graphically as the region created by the purple lines has a far greater area under the probability density function than the region formed by the green lines.
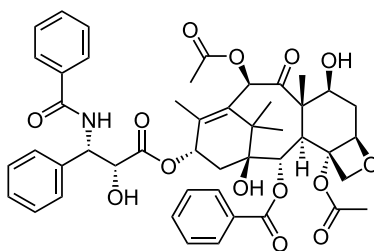
Figure 6: Chemical structure for paclitaxel

Part II
Application of Nanomaterials

The use of albumin protein nanoparticlces has provided a new delivery method for the highly effective chemotherapy drug, paclitaxel, in turn reducing side effects and toxicity caused by previous delivery schemes and increasing circulation half life around the body.

4   Paclitaxel

Paclitaxel is a chemotherapy drug in the taxane family which function as mitotic inhibitors. This involves the suppression of mitosis or cell division which is effective in treating cancer as constant cell mitosis is how cancer spreads throughout the body.

While taxanes are an effective cancer treatment, their use has proved difficult as they are not particularly soluble in water requiring a delivery vehicle in order to allow intraveneous application.

5   Previous Delivery Methods

As a result of the poor water solubility of taxanes and paclitaxel, a method for delivering a solution was required. Polyethoxylated castor oil (commercially known as Kolliphor EL, formerly Cremophor EL [CrEL]) combined with dehydrated ethanol provides a suitable formulation vehicle for many poorly water soluble and has been the standard for many forms of commercially available paclitaxel such as Taxol.

While this solution has proved to be an effective delivery mechanism there are significant side effects. CrEL has been shown to cause severe hypersensitivity reactions and peripheral neuropathy which are exacerbated by the high volumes of delivery agent which must be coadministered with the active ingredient[7]. The use of CrEL also affects the behaviour of paclitaxel when administered, manifesting as undesirable non-linear absorption, distribution, metabolism and excretion behaviour[8], typically referred to as a drug's pharmacokinetic characteristics.

6   Human Serum Albumin

Human serum albumin (HSA), sometimes referred to as blood albumin is the most frequently found protein in the human body[9] and is part of the albumin family of proteins. HSA is produced by the liver and performs important functions such as maintaining oncotic pressure in the blood vessels, ensuring the right levels of fluids are found between blood vessels and body tissues, and transporting hormones and fatty acids around the body.

Importantly for the application of drug delivery HSA along with the rest of the albumin proteins are water soluble and HSA effectively binds with both hydrophobic and hydrophilic chemicals[9]. Critically HSA has been shown to be nontoxic, non-immunogenic (provokes little response from the immune system), biocompatible and biodegradable[11] providing many advantages over Cremophor EL delivery.
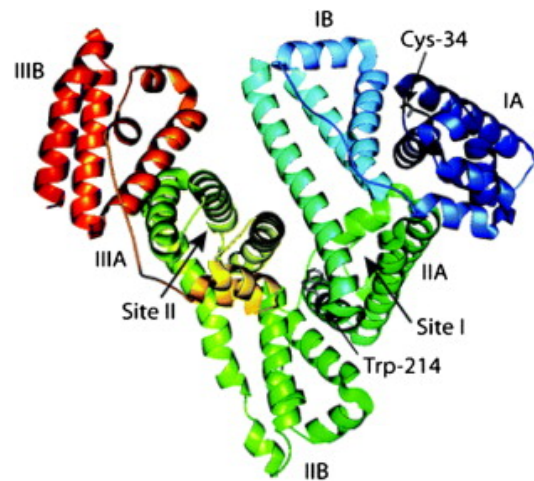
7   NAB-Paclitaxel

Word Count:

Figure 7: Crystal structure of human serum albumin with binding sites annotated[10]

References

[1] S. D. Gunapala, S. V. Bandara, J. K. Liu, J. M. Mumolo, S. B. Rafol, D. Z. Ting, A. Soibel, and C. Hill, "Quantum well infrared photodetector technology and applications", eng, *IEEE Journal of Selected Topics in Quantum Electronics*, vol. 20, no. 6, pp. 154,165, 2014-11, ISSN: 1077-260X.

[2] IoffeInstitute, *Nsm archive - physical properties of semiconductors*. [Online]. Available: http://matprop.ru/.

[3] Y. Takeda, A. Sasaki, Y. Imamura, and T. Takagi, "Electron mobility and energy gap of in 0.53 ga 0.47 as on inp substrate", eng, *Journal of Applied Physics*, vol. 47, no. 12, pp. 5405,5408, 1976-12, ISSN: 0021-8979.

[4] R. J. Nicholas, J. C. Portal, C. Houlbert, P. Perrier, and T. P. Pearsall, "An experimental determination of the effective masses for ga x in 1-x as y p 1-y alloys grown on inp", eng, *Applied Physics Letters*, vol. 34, no. 8, pp. 492,494, 1979, ISSN: 0003-6951.

[5] C. Hermann and T. P. Pearsall, "Optical pumping and the valence-band light-hole effective mass in ga x in 1-x as y p 1-y (y approx. 2.2x)", eng, *Applied Physics Letters*, vol. 38, no. 6, pp. 450,452, 1981, ISSN: 0003-6951.

[6] S. Y. Lin, C. T. Liu, D. C. Tsui, E. D. Jones, and L. R. Dawson, "Cyclotron resonance of two-dimensional holes in strained-layer quantum well structure of (100)in 0.20 ga 0.80 as/gaas", eng, *Applied Physics Letters*, vol. 55, no. 7, pp. 666,668, 1989-08-14, ISSN: 0003-6951.

[7] H Gelderblom, J Verweij, K Nooter, and A Sparreboom, "Cremophor el: The drawbacks and advantages of vehicle selection for drug formulation", eng, *European Journal of Cancer*, vol. 37, no. 13, pp. 1590,1598, 2001-09, ISSN: 0959-8049.

[8] A Sparreboom, O van Tellingen, W. J. Nooijen, and J. H. Beijnen, "Nonlinear pharmacokinetics of paclitaxel in mice results from the pharmaceutical vehicle cremophor el.", eng, *Cancer research*, vol. 56, no. 9, pp. 2112,2115, 1996-05-01, ISSN: 0008-5472. [Online]. Available: http://search.proquest.com/docview/78006535/.

[9] N. Lomis, S. Westfall, L. Farahdel, M. Malhotra, D. Shum-Tim, and S. Prakash, "Human serum albumin nanoparticles for use in cancer drug delivery: Process optimization and in vitro characterization.", eng, *Nanomaterials (Basel, Switzerland)*, vol. 6, no. 6, 2016-06-15, ISSN: 2079-4991. [Online]. Available: http://search.proquest.com/docview/1881262578/.

[10] S. Barbosa, P. Taboada, and V. Mosquera, "Chapter 32 - fibrillation and polymorphism of human serum albumin", in *Bio-nanoimaging*, V. N. Uversky and Y. L. Lyubchenko, Eds., Boston: Academic Press, 2014, pp. 345 –362, ISBN: 978-0-12-394431-3. DOI: https://doi.org/10.1016/B978-0-12-394431-3.00032-8. [Online]. Available: http://www.sciencedirect.com/science/article/pii/B9780123944313000328.

[11] A. Elzoghby, W. Samy, and N. Elgindy, "Albumin-based nanoparticles as potential controlled release drug delivery systems", English, *Journal Of Controlled Release*, vol. 157, no. 2, pp. 168,182, 2012-01-30, ISSN: 0168-3659.